Open access • Journal Article • DOI:10.1002/CNMA.201600337

Pentatwinned Cu Nanowires with Ultrathin Diameters below 20 nm and Their Use as Templates for the Synthesis of Au-Based Nanotubes — Source link

Ming Luo, Ming Luo, Ming Zhou, Robson Rosa da Silva ...+7 more authors

Institutions: The Wallace H. Coulter Department of Biomedical Engineering, Wuhan University, Brookhaven National Laboratory, Georgia Institute of Technology

Published on: 01 Mar 2017

Topics: Nanowire and Selected area diffraction

Pentatwinned Cu Nanowires with Ultrathin Diameters below 20 nm and Their Use as Templates for the Synthesis of Au-Based Nanotubes

M. Luo, J. Tao

Submitted to CHEMNANOMAT

March 2017

Condensed Matter Physics and Materials Science Department

Brookhaven National Laboratory

U.S. Department of Energy
USDOE Office of Science (SC),
Basic Energy Sciences (BES) (SC-22)

DISCLAIMER

Penta-Twinned Cu Nanowires with Ultrathin Diameters below 20 nm and Their Use as Templates for the Synthesis of Au-Based Nanotubes

Ming Luo,+[a,b] Ming Zhou,+[a] Robson Rosa da Silva,[a] Jing Tao,[c] Legna Figueroa-Cosme,[d] KyleD. Gilroy,[a] Hsin-Chieh Peng,[d] Zhike He,[b] and Younan Xia*[a,d]

[a] *The Wallace H. Coulter Department of Biomedical Engineering, Georgia Institute of Technology and Emory University, Atlanta, Georgia 30332, United States*

[b] *Key Laboratory of Analytical Chemistry for Biology and Medicine, Ministry of Education, College of Chemistry and Molecular Sciences, Wuhan University, Wuhan 430072, P. R. China*

[c] *Condensed Matter Physics and Materials Science Department, Brookhaven National Laboratory, Upton, New York 11973, United States*

[d] *School of Chemistry and Biochemistry, School of Chemical and Biomolecular Engineering, Georgia Institute of Technology, Atlanta, Georgia 30332, United States*

+ *These two authors contributed equally to this work.*

* *Address correspondence to younan.xia@bme.gatech.edu.*

Abstract

We report a one-pot method for the facile synthesis of Cu nanowires in high purity, together with ultrathin diameters well below 20 nm. Selected area electron diffraction and high-resolution transmission electron microscopy studies confirm that the Cu nanowires are grown along the <110> direction to give a penta-twinned, one-dimensional nanostructure, enclosed by five {100} facets on the side surface. A systematic study further indicates that it is critical to conduct the synthesis under an argon atmosphere in order to improve the purity and uniformity of the nanowires while keeping their diameters thinner than 20 nm. We also demonstrate the use of these nanowires as sacrificial templates for the synthesis of Au-based nanotubes through a galvanic replacement process.

Keywords: copper · argon protection· reduction kinetics · nanowires · hollow nanostructures

Table of Contents

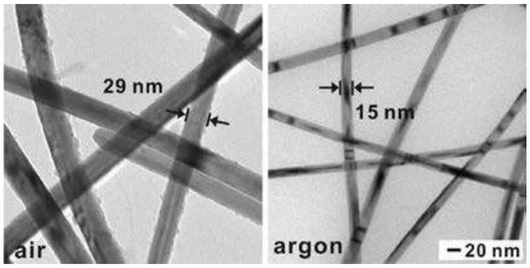

Introduction

Transparent conductors are used in a wide variety of applications, including low-emissivity windows, flat-panel displays, touch screens, and thin-film solar cells.[1] For these applications, both low resistance and high transmittance are always desirable. Indium tin oxide (ITO) is the most commonly used transparent conductor because it can be deposited as thin films at relatively low temperatures and it is also easier to pattern this material than other conducting oxides having comparable conductivity and transmittance.[2] However, the brittleness and the high material cost associated with ITO have made it necessary to find alternative materials for the fabrication of flexible transparent conductors.[3] To this end, films consisting of carbon nanotubes and graphene have been extensively explored as possible replacements, but their performance still need to be improved in order to beat ITO in terms of conductivity and transparency.[4-7] On the other hand, it has been reported that flexible films could be fabricated from Ag nanowires to give conductivity and transmittance comparable to those of ITO, albeit Ag and In are similar in terms of price and scarcity.[3,8,9] In comparison, Cu is only 6% less conductive than Ag while it is 1000 times more abundant and 100 times less expensive relative to both Ag and In.[3] As a result, Cu nanowires has recently emerged as a promising candidate material for the production of low-cost, flexible, and transparent conductors.[10]

Both experimental measurements and modeling studies have demonstrated that a network comprised of metal nanowires with a thinner diameter would outperform a counterpart consisting of thicker nanowires in terms of transmittance, especially in the case of high conductivity, at which point the number of connections between the nanowires will limit the sheet resistance of the network.[9,11-13] As such, switching to thinner and longer metal nanowires is anticipated to significantly increase the conductivity of the network while maintaining high transmittance. Accordingly, one will be able to greatly increase the conductivity and related performance of such a network at a given transmittance by simply reducing the diameter of the nanowires.

A number of protocols have been reported for the chemical syntheses of Cu nanowires.[14-22] Among them, solution-phase methods involving the mediation of alkylamine or alkyldiamine have been most extensively explored. In particular, ethylenediamine (EDA) has been employed as a coordination ligand to promote the growth of long Cu nanowires in high yield. Essentially, the synthesis involves the reduction of a Cu(II) precursor by hydrazine under alkaline conditions in the presence of EDA in an aqueous solution. Zeng reported the first EDA-mediated synthesis of Cu nanowires and the products were typically 90–120 nm in diameter and 40–50 μm in length.[14] Wiley further modified Zeng's approach and scaled up the synthesis by 100 times.[15] The Cu nanowires prepared using the modified method had a diameter of about 35 nm, together with lengths up to 80 μm. Different from the EDA-based synthesis, the alkylamine-mediated synthesis was typically carried out under a neutral or moderately alkaline condition at a higher temperature. To this end, Shi reported a hydrothermal route to Cu nanowires by reducing $CuCl_2$ with octadecylamine in water at 120–180 ^{o}C.[18] The Cu nanowires produced using this method had a broad distribution of diameters in the range of 30–100 nm and lengths up to 40 μm. Peng replaced the octadecylamine with oleyamine as reductant, and introduced Ni(II) as a catalyst for the reduction of Cu(II).[19] These modifications reduced the average diameter of the Cu nanowires down to 16 nm, while the lengths were kept at 40 μm. However, this method requires the use of a pretty high temperature of 175 ^{o}C, together with an organic reagent. In an early study, our group reduced the reaction temperature to 100 ^{o}C by using hexadecylamine (HDA) as a capping agent in an aqueous solution to produce Cu nanowires with an average diameter of 24 nm and lengths ranging from tens to hundreds of micrometers.[21] Despite these prior reports, it still remains challenging to produce Cu nanowires with diameters well below 20 nm, under mild conditions, together with high purity to investigate their optical/electrical properties and related applications.

In the present work, we report a facile and reliable approach to prepare Cu nanowires with an average diameter around 15 nm and in high purity. In this synthesis, argon protection was found to play a pivotal role in reducing the diameter and improving the purity of the resultant Cu nanowires. Our mechanistic study indicates that oxygen could be removed from the surface of the Cu nanostructures under argon protection, leading to reduction in diameter for the nanowires. In addition, oxidative etching was suppressed when the synthesis was conducted under an argon atmosphere, which could increase the percentage of multiply twinned seeds at the early stage and thus improving the yield and purity of Cu nanowires in the final products. The reduction kinetics was also accelerated under argon protection to greatly shorten the reaction time. Using the as-prepared Cu nanowires as templates, we also demonstrated the synthesis of Au-based nanotubes *via* a galvanic replacement reaction.

Results and Discussion

In a typical synthesis, $CuCl_2$, glucose, and HDA were mixed in water hosted in a glass vial and capped. The mixture was then magnetically stirred at room temperature overnight. Different from our previous work, argon was blown through the solution to remove oxygen from the system. Under ambient conditions, the dissolved oxygen concentration in water is typically around 8 mg/L,[23,24] and blowing argon through the solution can decrease the concentration roughly 200 folds to 30 μg/L.[23] After blowing with argon, the vial was immediately capped and transferred into an oil bath held at 120 °C and heated for 3 h under magnetic stirring.[21] As the reaction proceeded, the solution gradually changed its color from blue to red-brown (see the photographs in Figure S1), implying the reduction of Cu(II) ions by glucose for the formation of Cu nanostructures.

Figure 1, A and B, shows representative transmission electron microscopy (TEM) images of the as-obtained product, clearly indicating that the nanowires had a uniform lateral dimension along the long axis of each nanowire, as well as a uniform distribution in diameter across the sample. The nanowires had an average diameter of 15 nm as calculated from 50 nanowires randomly selected from a number of TEM images (Figure 1C). The lengths of the Cu nanowires varied in the range of several tens to hundreds of micrometers. These ultrathin nanowires showed excellent flexibility and some of them could endure nearly 180° bending without breaking into shorter segments (Figure 1D). Compared with the Cu nanowires obtained under air (Figure S2, which had an average diameter of 29 nm), the Cu nanowires prepared under argon protection showed drastic reduction in diameter. In addition, the Cu nanostructures with irregular shapes also disappeared from the final products, indicating the marked improvement in both yield and purity for the Cu nanowires when conducted under an argon atmosphere.

We further used selected area electron diffraction (SAED) and high-resolution TEM (HR-TEM) analysis to characterize the morphology and structure of the as-prepared Cu nanowires. Figure 2, A and B, schematically illustrates two Cu nanowires with different orientations relative to the electron beam (indicated by arrows). Figure 2, C and D, shows the typical SAED patterns recorded from the Cu nanowires. Both patterns indicate that the Cu nanowires were not a single crystal because the diffraction spots could not be assigned to any particular simple pattern associated with face-centered cubic (*fcc*) Cu. Most of the diffraction spots in Figure 2C could be indexed as the diffractions along the $[1\bar{1}\bar{2}]$ and [001] zone axes (Figure 2A), while those in

Figure 2D could be assigned to the diffractions along the $[1\bar{1}0]$ and $[1\bar{1}\bar{1}]$ zone axes (Figure 2B), consistent with the previous results reported for penta-twinned nanowires.[25] Figure 2, E and F, shows HRTEM images recorded from the two Cu nanowires, respectively. When the direction of the electron beam was perpendicular to the bottom side of the nanowire (Figure 2E), two sets of fringes with lattice spacing of 0.21 nm and 0.13 nm were observed, corresponding to the {111} and {220} planes of *fcc* Cu, respectively. Figure 2F shows the HRTEM image taken from a Cu nanowire oriented with one of its side faces parallel to the electron beam. The fringes with lattice spacing of 0.21, 0.18, and 0.13 nm could be indexed to the {111}, {200}, and {220} planes of *fcc* Cu. Based on the results of SAED patterns and HRTEM analyses, it can be concluded that the Cu nanowires had a penta-twinned structure bound by five {100} side faces, with their longitudinal direction along <110>. According to previous work, such a penta-twinned structure is instrumental to the achievement of high electrical conductivity and high mechanical strength for the Cu nanowires.[26]

We further used X-ray diffraction (XRD) and X-ray photoelectron spectroscopy (XPS) to characterize the composition of the as-prepared Cu nanowires. Figure 3A shows an XRD pattern recorded from a thin film of the Cu nanowires drop-cast on a glass substrate. The three peaks at $2\theta = 43.4$, 51.2, and 74.2^{o} could be indexed to the diffractions from {111}, {200}, and {220} planes of *fcc* Cu (JCPDS #03-1018). The XRD peak positions were in good agreement with the values reported in literature, confirming highly crystallinity of the Cu nanowire.[21] According to our previous reports, both HDA and Cl^{-} ions play an important role in controlling the formation of penta-twinned Cu nanorods and nanowires.[21,27] As shown in Figure S2, C 1s, N 1s, and Cl 2p peaks could all be observed in the XPS survey spectrum, indicating the existence of Cl^{-} ions and HDA molecules on the surface of the as-obtained Cu nanowires. The O 2p peak was also found in the survey spectrum. Despite the protection by a HDA sheath, the Cu atoms on the surface were oxidized to form an ultrathin layer of Cu_2O or CuO according to our previous report.[21]

Figure 3B shows the UV–vis–NIR extinction spectrum recorded from an aqueous suspension of the as-obtained Cu nanowires, indicating the existence of a plasmon resonance peak at 560 nm. It is well known that one-dimensional nanostructures comprised of Au, Ag, and Cu exhibit both transverse and longitudinal localized surface plasmon resonance (LSPR) peaks, which originate from the light-induced collective oscillations of conduction electrons parallel to the short and long axes, respectively.[27-32] In general, the transverse mode appears at a shorter wavelength than the longitudinal mode. We thus assign the peak at 560 nm to the transverse LSPR mode of the Cu nanowires. Similar to Ag nanowires, only the transverse peak could be observed in the extinction spectrum because the longitudinal peak should have been shifted to the infrared region due to the extremely large aspect ratios of the Cu nanowires.[33-35]

We attributed the thinning of Cu nanowires to the removal of oxygen from the reaction system by argon. It is well documented that molecular oxygen can adsorb and dissociate on Cu surface.[36-41] According to our previous report, HDA is an effective capping agent for the {100} facets on Cu nanostructures, which could protect the underlying Cu from being oxidized.[21] While the side faces were protected by HDA, the oxygen could still attack the ends of each nanowire, which were bound by {111} facets, retarding the deposition of Cu atoms for axial growth. A plausible mechanism is illustrated in Figure 4. Under air, atomic oxygen preferred to adsorb on the {111} facets, blocking the continuous deposition of Cu atoms onto the ends and thereby promoting lateral growth. With the introduction of argon, the O_2 was removed from the reaction system. As a result, the deposition rate on the {111} facets was accelerated owing to the elimination of oxygen from the system. Consequently, the diameter of the Cu nanowires prepared under argon protection would become much thinner. As established in literature for a number of noble metals, a penta-twinned nanorod or nanowire originates from a decahedral seed with a multiply twinned structure.[33] To this end, oxidative etching could affect the yield of the multiply twinned seeds relative to other types of seeds in the initial stage of a synthesis.[42-44] The application of argon protection could remove oxygen from the reaction system and thus suppress oxidative etching. As a result, the multiply twinned seeds could be saved from oxidation and etching, leading to improvement in yield and purity for the Cu nanowires.

We also noticed that the reaction time was greatly shortened if conducted under an argon atmosphere. In the presence of dissolved oxygen, we hypothesize that there exist *two* competing reaction pathways (as shown in Figure 4) that simultaneously counteract one another. The faster reaction is the reduction of Cu(II) into Cu(0) atoms by the reductant (glucose). These newly formed atoms contribute to the nucleation and growth of the nanowires. Counteracting this reaction pathway is the oxidation of Cu(0) atoms back into Cu(I) or Cu(II) by the dissolved oxygen. To test this hypothesis, we removed the dissolved oxygen from the reaction system by blowing argon through the precursor solution. Then, by measuring the percent conversions of Cu(II) ions to Cu(0) atoms as a function of the reaction time using inductively coupled plasma mass spectrometry (ICP-MS), we found that the conversion of Cu(II) ions to Cu(0) atoms could be completed within a much shorter period of time relative to the case under air (Figure 5), indicating a faster reduction rate under argon protection.

Nanostructures with hollow porous walls and interiors have many interesting properties, such as reduced densities, enlarged surface areas, and tunable compositions in comparison with their solid counterpart.[45-48] When used as sacrificial templates, Cu nanostructures are advantageous over Ag nanostructures.[49] For example, the standard reduction potential of Cu(II)/Cu pair (0.34 V *versus* the standard hydrogen electrode, SHE) is much lower than that of Ag(I)/Ag pair (0.8 V *versus* SHE), which could provide a stronger driving force for galvanic replacement with a broader range of salt precursors. Meanwhile, the Cu(II) ions generated during the replacement process would remain in the solution as a soluble byproduct (while AgCl has a relatively lower solubility), eliminating the need to purity the products. Most significantly, the abundance of Cu is 1000 times greater than Ag in the earth's crust, while the cost is only one percent of that of Ag, making Cu nanostructures a perfect candidate for applications as a sacrificial template.[15] There are only a few reports on the galvanic replacement involving Cu-based nanostructures.[49,50] In a proof-of-concept experiment, here we employed the as-prepared Cu nanowires, such as those shown in Figure 1, as sacrificial templates to generate Au-based nanotubes. The preparation of such hollow nanostructures involved the galvanic replacement reaction between $AuCl_4^-$ ions and Cu nanowires. After titrating with a sufficient amount of $HAuCl_4$, $Au_{58}Cu_{42}$ nanotubes having highly porous walls with and slightly enlarged diameters were obtained (Figure 6). Since the galvanic replacement reaction can be performed with any metal precursor having a higher redox potential than Cu metal, hollow metal nanostructures with a variety of other compositions can also be obtained by simply switching to other metal salt precursors (*e.g.*, Pd^{2+} or Pt^{2+}).

Conclusion

We have demonstrated a facile approach to the synthesis of Cu nanowires in high purity, together with ultrathin diameters well below 20 nm. Both SAED patterns and HR-TEM images results confirm that the as-prepared Cu nanowires had a penta-twinned structure bound by {111} facets on the side surface, with their longitudinal direction along <110>. The XPS data indicate that both HDA molecules and Cl^- ions had adsorbed onto the surface of the Cu nanowires. Our mechanistic studies suggest that argon protection was critical to the reduction in diameter for the nanowires, as well as the improvement in yield and purity. Owing to the removing of oxygen from the reaction system, the reaction kinetics was increased, and then shortened the reaction time. When the oxygen on the two ends of the Cu nanowires were removed under an argon atmosphere, the axial growth was accelerated yield thinner Cu nanowires. In the meantime, the argon atmosphere could suppress oxidative etching, improving the yield and purity of the Cu nanowires. In a proof-of-concept experiment, the Cu nanowires were further converted into Au-based hollow nanostructures. We believe that the synthesis of ultrathin Cu nanowires will greatly promote their widespread use in applications related to flexible electronics, display, and catalysis.

Experimental Section

Chemicals and materials: Hexadecylamine (HDA, 98%), copper(II) chloride dihydrate ($CuCl_2 \cdot 2H_2O$, 99.0%), poly(vinyl pyrrolidone) (PVP, $M_w \approx 55{,}000$), glucose ($C_6H_{12}O_6$, 96%), and gold(III) chloride trihydrate ($HAuCl_4 \cdot 3H_2O$, 99.9%) were all obtained from Sigma-Aldrich. Ethylene glycol (EG) was purchased from J. T. Baker. Ethanol (200 proof) was obtained from Pharmco Products. All the chemicals were obtained from Sigma-Aldrich and used as received. Deionized (DI) water of 18.2 MΩ·cm in resistivity was used throughout the experiments.

Synthesis of Cu nanowires: In a standard synthesis of Cu nanowires, an aqueous solution (10 mL) containing HDA (180 mg), glucose (50 mg), and $CuCl_2 \cdot 2H_2O$ (21 mg) was magnetically stirred at room temperature overnight. Note that the HDA might not completely dissolve, and small white clumps of HDA could be present in the precursor solution after mixing. This should not affect the outcome of a synthesis. The mixture was magnetically stirred for 5 min under argon atmosphere (with argon blowing through the solution surface). The vial was then capped and transferred into an oil bath held at 120 ^{o}C for 3 h under magnetic stirring. The product was collected with ethanol by centrifugation at 12,000 rpm, followed by washing with hexane and then ethanol to remove excess HDA, and finally re-dispersed in EG (50 mL).

Synthesis of Au-based hollow nanostructures: The Au-based hollow nanostructures were synthesized through a galvanic replacement reaction between the Cu nanowires and $AuCl_4^-$ ions in EG. In a typical synthesis, PVP (30 mg) was added into a solution of the as-prepared Cu nanowires suspended in EG (10 mL) and hosted in a 50 mL flask, and then magnetically stirred for 10 min at room temperature. Subsequently, a solution of $HAuCl_4$ in EG (1.0 mL, 1.0 mM) was pumped into the above solution at the rate of 0.1 mL/min. After that, the reaction was continued for additional 30 min. The product was collected by centrifugation, washed three times with ethanol, and then re-dispersed in water.

Characterization: TEM images were taken using a Hitachi HT7700 microscope operated at 120 kV by drop casting the nanoparticle dispersions on carbon-coated Cu grids and drying under ambient conditions. HR-TEM and SAED analyses were performed using JEOL 2100F microscope (JEOL, Tokyo, Japan) operated at 200kV. UV-vis-NIR absorption spectra were recorded with a Lambda 750 spectrometer (Perkin-Elmer). The concentration of elemental Cu was determined using ICP-MS (NexION 300Q, Perkin-Elmer). XRD patterns were recorded using an X'Pert PRO Alpha-1 diffractometer (PANalytical, Almelo, The Netherlands) with a 1.8 kW ceramic copper tube source. The XPS data were recorded using a Thermo K-Alpha spectrometer with an Al Kα source (eV).

Acknowledgements

This work was supported in part by a research grant from NSF (DMR-1506018) and startup funds from the Georgia Institute of Technology. As jointly supervised Ph.D. candidates from Wuhan University and Chongqing University, M.L. and M.Z. were also partially supported by fellowship from the China Scholarship Council.

Supporting Information: Supporting Information is available from the Wiley Online Library or from the author.

REFERENCES

[1] *Indium Tin Oxide and Alternative Transparent Conductor Markets*, NanoMarkets, LC, **2009**.

[2] R. G. Gordon, *MRS Bull*. **2000**, *25*, 52–57.

[3] U.S. Geological Survey, Mineral Commodity Summaries. **2015**.

[4] L. Hu, D. S. Hecht, G. Grüner, *Chem. Rev.* **2010**, *110,* 5790–5844.

[5] Z. Wu, Z. Chen, X. Du, J. M. Logan, J. Sippel, M. Nikolou, K. Kamaras, J. R. Reynolds, D.

B. Tanner, A. F. Hebard, A. G. Rinzler. *Science* **2004**, *305*, 1273–1276.

[6] S. Bae, H. Kim, Y. Lee, X. Xu, J.-S. Park, Y. Zheng, J. Balakrishnan, T. Lei, H. R. Kim, Y. I. Song, Y.-J. Kim, K. S. Kim, B. Özyilmaz, J.-H. Ahn, B. H. Hong, S. Iijima, *Nat. Nanotechnol.* **2010**, *5*, 574–578.

[7] J. H. Lee, D. W. Shin, V. G. Makotchenko, A. S. Nazarov, V. E. Fedorov, Y. H. Kim, J.-Y. Choi, J. M. Kim, J.-B. Yoo, *Adv. Mater.* **2009**, *21*, 4383–4387.

[8] M. Song, D. S. You, K. Lim, S. Park, S. Jung, C. S. Kim, D.-H. Kim, D.-G. Kim, J.-K. Kim, J. Park, Y.-C. Kang, J. Heo, S.-H. Jin, J. H. Park, J.-W. Kang, *Adv. Funct. Mater.* **2013**, *23*, 4177–4184.

[9] L. Hu, H. S. Kim, J.-Y. Lee, P. Peumans, Y. Cui, *ACS Nano* **2010**, *4*, 2955–2963.

[10] S. Ye, A. R. Rathmell, Z. Chen, I. E. Stewart, B. J. Wiley, *Adv. Mater.* **2014**, *26*, 6670–6687.

[11] Y. C. Lu, K. S. Chou, *Nanotechnology* **2010**, *21*, 215707.

[12] S. M. Bergin, Y.-H. Chen, A. R. Rathmell, P. Charbonneau, Z.-Y. Li, B. J. Wiley, *Nanoscale* **2012**, *4*, 1996–2004.

[13] R. M. Mutiso, M. C. Sherrott, A. R. Rathmell, B. J. Wiley, K. I. Winey, *ACS Nano* **2013**, *7*, 7654–7663.

[14] Y. Chang, M. L. Lye, H. C. Zeng, *Langmuir* **2005**, *21,* 3746–3748.

[15] A. R. Rathmell, S. M. Bergin, Y.-L. Hua, Z.-Y. Li, B. J. Wiley, *Adv. Mater.* **2010**, *22*, 3558–3563.

[16] S. Ye, A. R. Rathmell, I. E. Stewart, Y.-C. Ha, A. R. Wilson, Z. Chen, B. J. Wiley, *Chem. Commun.* **2014**, *50*, 2562–2564.

[17] S. Ye, A. R. Rathmell, Y.-C. Ha, A. R. Wilson, B. J. Wiley, *Small* **2014**, *10*, 1771–1778.

[18] Y. Shi, H. Li, L. Chen, X. Huang, *Sci. Technol. Adv. Mater.* **2005**, *6*, 761–765.

[19] H. Guo, N. Lin, Y. Chen, Z. Wang, Q. Xie, T. Zheng, N. Gao, S. Li, J. Kang, D. Cai, D.-L. Peng, *Sci. Rep.* **2013**, *3*, 2323.

[20] M. Mohl, P. Pusztai, A. Kukovecz, Z. Konya, J. Kukkola, K. Kordas, R. Vajtai, P. M. Ajayan, *Langmuir* **2010**, *26*, 16496–16502.

[21] M. Jin, G. He, H. Zhang, J. Zeng, Z. Xie, Y. Xia, *Angew. Chem. Int. Ed.* **2011**, *50*, 10560–10564.

[22] D. Zhang, R. Wang, M. Wen, D. Weng, X. Cui, J. Sun, H. Li, Y. Lu, *J. Am. Chem. Soc.* **2012**,

134, 14283–14286.

[23] E. Menumerov, R. A. Hughes, S. Neretina, *Nano Lett.* **2016**, *16*, 7791−7797.

[24] Z. Zhang, Z. Chen, F. Cheng, Y. Zhang, L. Chen, *Analyst* **2016**, *141*, 2955−2961.

[25] I. Lisiecki, A. Filankembo, H. Sack-Kongehl, K. Weiss, M.-P. Pileni, J. Urban, *Phys. Rev. B* **2000**, *61*, 4968–4974.

[26] L. Lu, Y. Shen, X. Chen, L. Qian, K. Lu, *Science* **2004**, *304*, 422–426.

[27] M. Luo, A. Ruditskiy, H.-C. Peng, J. Tao, L. Figueroa-Cosme, Z. He, Y. Xia, *Adv. Funct. Mater*. **2016**, *26*, 1209–1216.

[28] B. Nikoobakht, M. A. El-Sayed, *Chem. Mater.* **2003**, *15,* 1957–1962.

[29] M. Rycenga, C. M. Cobley, J. Zeng, W. Li, C. H. Moran, Q. Zhang, D. Qin, Y. Xia, *Chem. Rev*. **2011**, *111*, 3669–3712.

[30] M. Luo, H. Huang, S.-I. Choi, C. Zhang, R. R. da Silva, H.-C. Peng, Z.-Y. Li, J. Liu, Z. He, Y. Xia, *ACS Nano* **2015**, *9*, 10523–10532.

[31] B. Pietrobon, M. McEachran, V. Kitaev, *ACS Nano* **2009**, *3*, 21−26.

[32] Y. Xu, Y. Zhao, L. Chen, X. Wang, J. Sun, H. Wu, F. Bao, J. Fan, Q. Zhang, *Nanoscale* **2015**, *7*, 6790–6797.

[33] R. R. da Silva, M. Yang, S.-I. Choi, M. Chi, M. Luo, C. Zhang, Z.-Y. Li, P. H. C. Camargo, S. J. L. Ribeiro, Y. Xia, *ACS Nano* **2016**, *10*, 7892–7900.

[34] Y. Sun, Y. Xia, *Adv. Mater*. **2002**, *14*, 833–837.

[35] Y. Sun, Y. Yin, B. T. Mayers, T. Herricks, Y. Xia, *Chem. Mater.* **2002,** *14,* 4736–4745.

[36] Y. Xu, M. Mavrikakis, *Surf. Sci.* **2001**, *494*, 131–144.

[37] T. Matsumoto, R. A. Bennett, P. Stone, T. Yamada, K. Domen, M. Bowker, *Surf. Sci.* **2001**, *471*, 225–245.

[38] Z. X. Wang, F. H. Tian, *J. Phys. Chem. B* **2003**, *107*, 6153–6161.

[39] W. Jacob, V. Dose, A. Goldmann, *Appl. Phys. A* **1986**, *41*, 145–150.

[40] N. Ikemiya, T. Kubo, S. Hara, *Surf. Sci*. **1995**, 323, 81–90.

[41] K. H. Schulz, D. F. Cox, *Phys. Rev. B* **1991**, *43*, 1610–1621.

[42] B. Wiley, Y. Xiong, Z. Li, Y. Yin, Y. Xia, *Nano Lett*. **2006**, *6*, 765–768.

[43] B. Wiley, T. Herricks, Y. Sun, Y. Xia, *Nano Lett*. **2004**, *4*, 2057–2057.

[44] Y. Xiong, J. Chen, B. Wiley, Y. Xia, *J. Am. Chem. Soc*. **2005**, *127*, 7332–7333.

[45] J. Chen, B. J. Wiley, J. McLellan, Y. Xiong, Z.-Y. Li, Y. Xia, *Nano Lett*. **2005**, *5*, 2058–2062.

[46] J. Chen, J. M. McLellan, A. Siekkinen, Y. Xiong, Z.-Y. Li, Y. Xia, *J. Am. Chem. Soc*, **2006**, *5*, 14776–14777.

[47] X. Wang, M. Figueroa-Cosme, X. Yang, M. Luo, J. Liu, Z. Xie, Y. Xia, *Nano Lett*. **2016**, *16*, 1467–1471.

[48] H. Jing, H. Wang, *Chem. Mater*. **2015**, *27*, 2172−2180.

[49] S. Xie, M. Jin, J. Tao, Y. Wang, Z. Xie, Y. Zhu, Y. Xia, *Chem. Eur. J.* **2012**, *18*, 14974–14980.

[50] M. Mohl, D. Dobo, A. Kukovecz, Z. Konya, K. Kordas, J. Wei, R. Vajtai, P. M. Ajayan, *J. Phys. Chem. C* **2011**, *115*, 9403–9409.

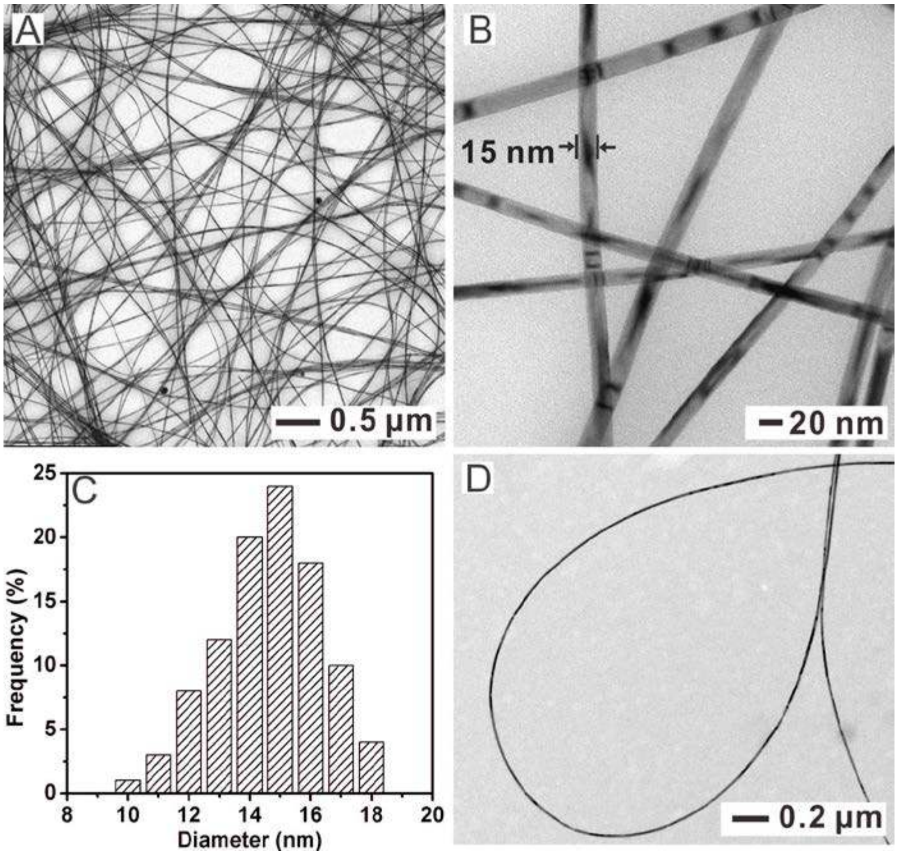

Figure 1. Characterization of Cu nanowires synthesized using the standard procedure. (A, B, D) TEM images of the as-prepared Cu nanowires, and (C) diameter distribution of the nanowires shown in (A).

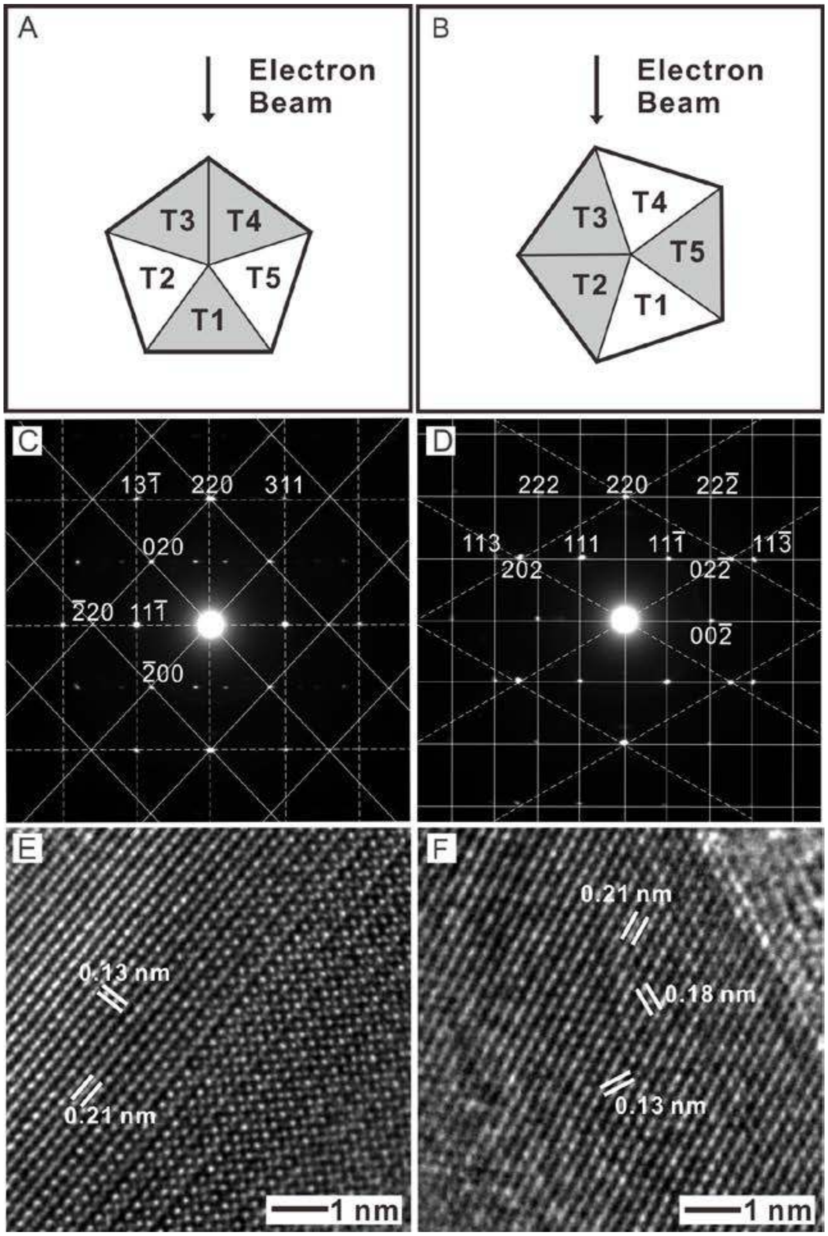

Figure 2. Characterizations of two individual Cu nanowires: (A, B) schematic illustrations of the Cu nanowires relative to the electron beam, (C, D) SAED patterns, and (E, F) high-resolution TEM images.

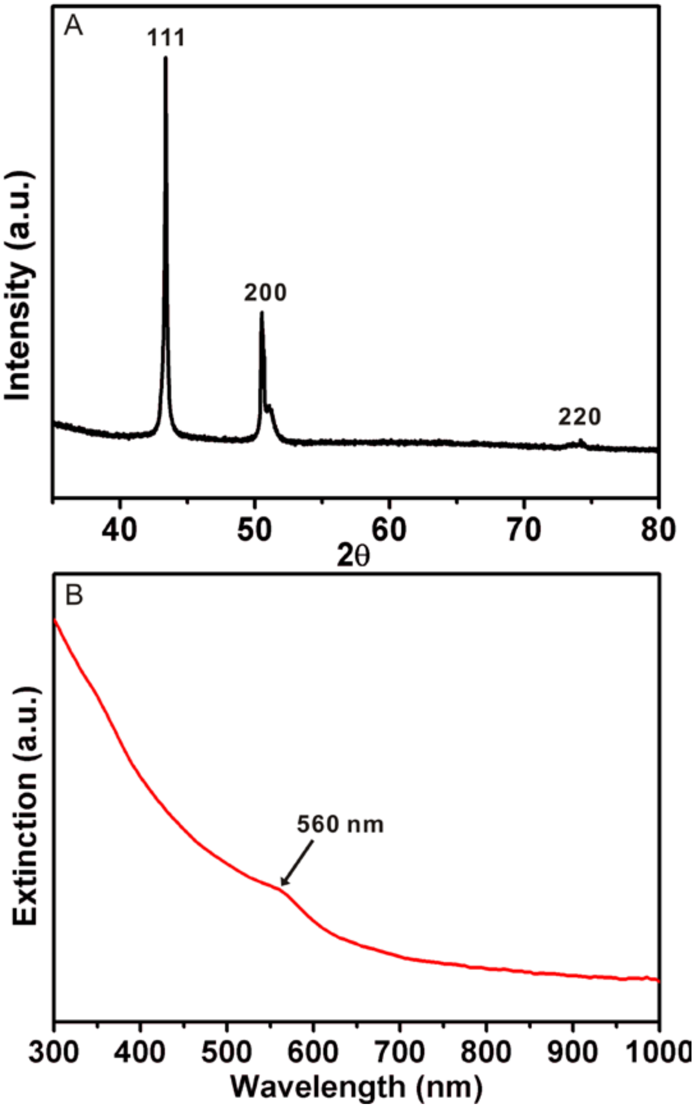

Figure 3. (A) Powder XRD pattern of Cu nanowires, confirming their *fcc* structure. (B) UV-vis-NIR extinction spectrum recorded from an aqueous suspension of the Cu nanowires.

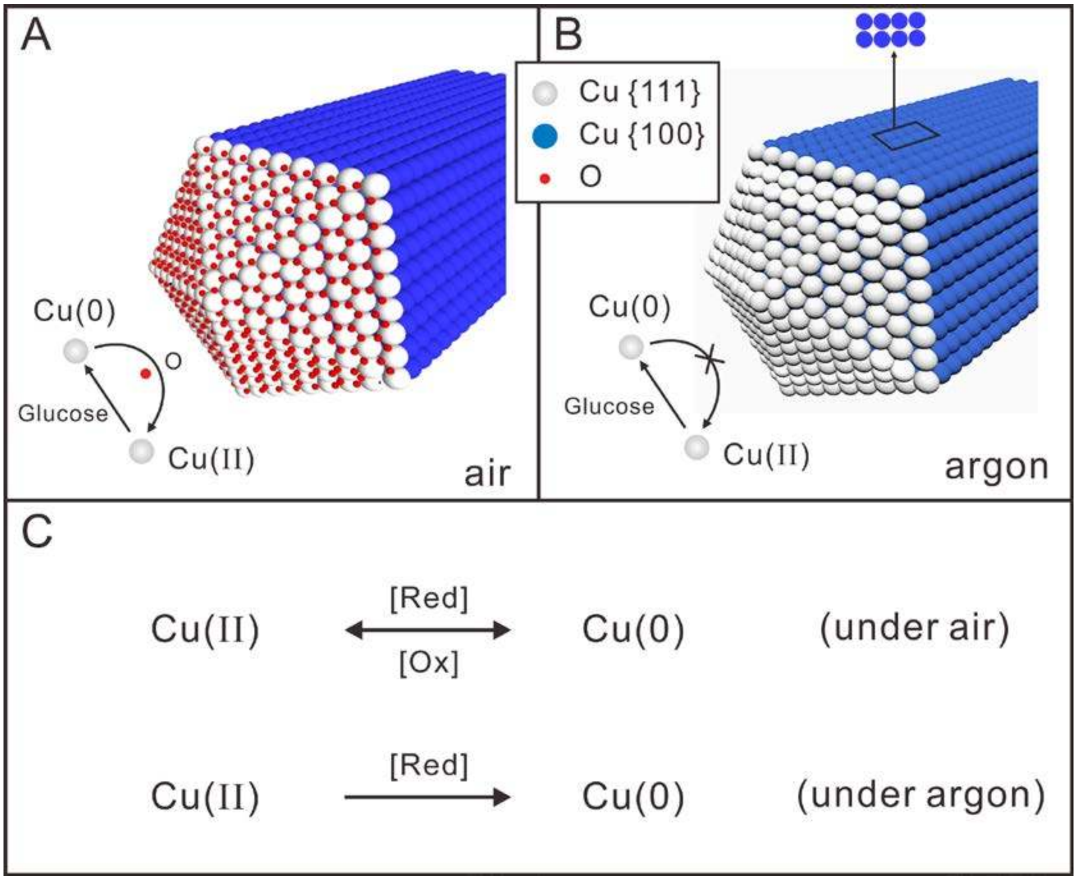

Figure 4. Schematic illustrations of the growth mechanisms responsible for the formation of Cu nanowires under (A) air and (B) argon atmospheres. (C) Proposed chemical reactions in air and under the protection of argon.

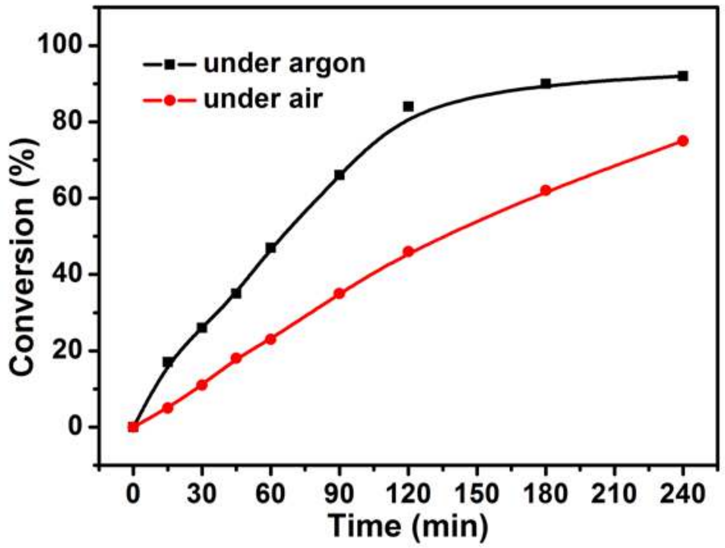

Figure 5. Plots showing the conversions of Cu(II) ions into Cu(0) atoms under air and argon atmospheres, respectively, as a function of reaction time.

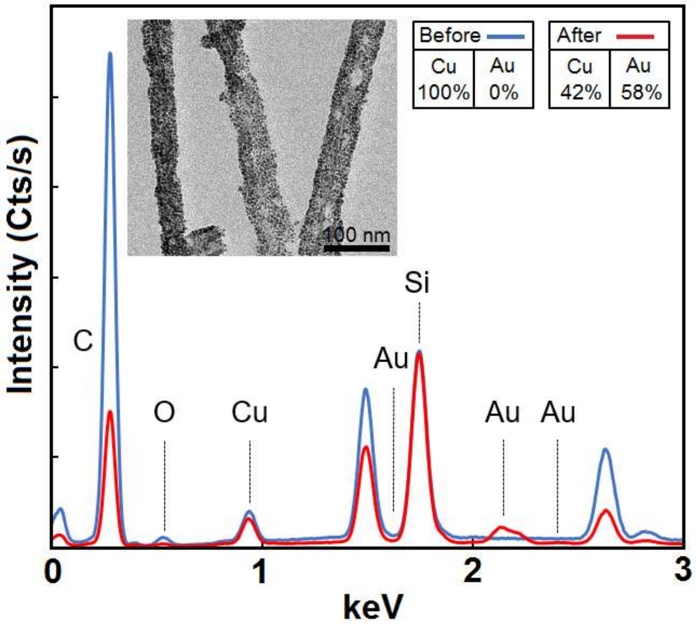

Figure 6. Energy dispersive spectrometry (EDS) spectra of the Cu-nanowires (blue line) and Au-based nanotubes (red line), indicating that the composition changes from pure Cu to $Au_{58}Cu_{42}$ after the galvanic replacement reaction with Au(III). The inset shows a typical TEM image of the Au-based hollow nanostructures.

Penta-Twinned Cu Nanowires with Ultrathin Diameters below 20 nm and Their Use as Templates for the Synthesis of Au Nanotubes

Ming Luo, Ming Zhou, Robson Rosa da Silva, Jing Tao, Legna Figueroa-Cosme, Kyle D. Gilroy, Hsin-Chieh Peng, Zhike He, and Younan Xia*

*Corresponding authors: younan.xia@bme.gatech.edu

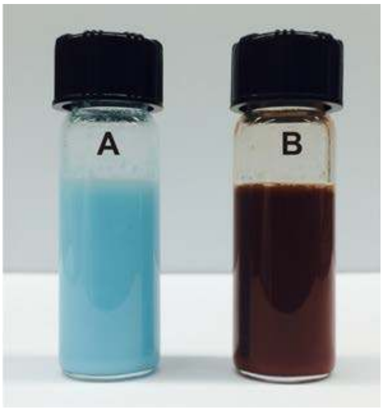

Figure S1. Photographs of (A) the aqueous reaction solution and (B) the as-prepared suspension of Cu nanowires.

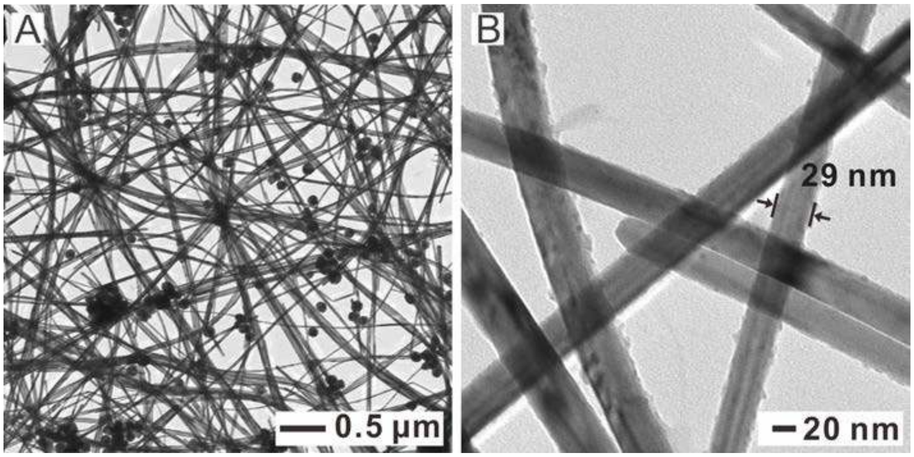

Figure S2. TEM images of the Cu nanowires synthesized under air while other conditions were kept the same as in the standard procedure.

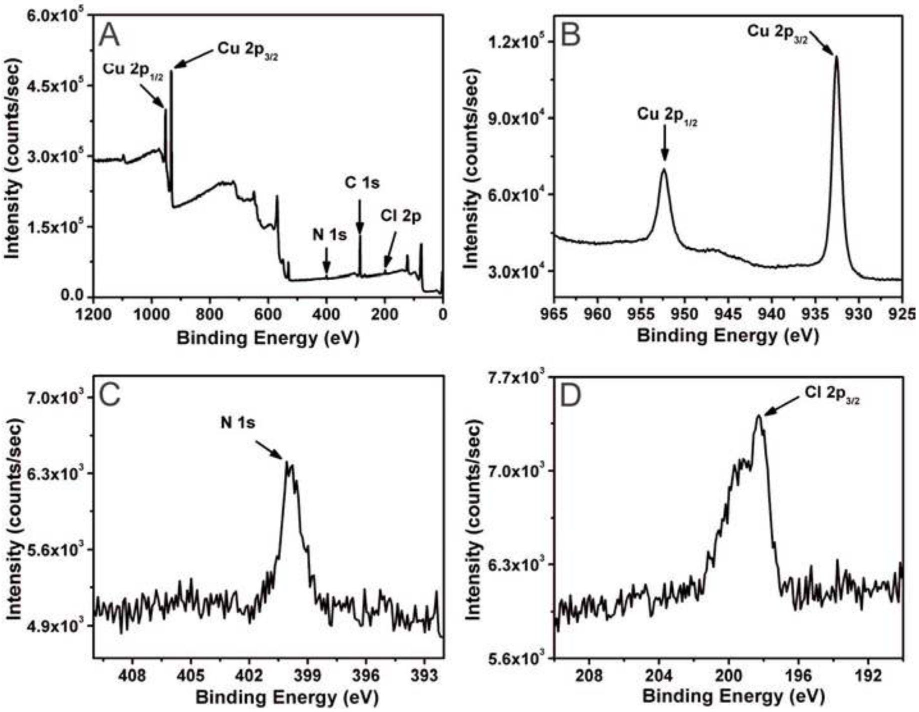

Figure S3. XPS spectra of the repeatedly washed Cu nanowires: (A) a survey scan, (B) Cu 2p, (C) N 1s, and (D) Cl 2p energy regions, respectively.